



Techno Science Africana Journal

Journal homepage: www.technoscienceafricana.com



LUMINESCENCE PROPERTIES OF (70-X) Zn_230SiO_4 DOPED WITH Sm^{3+} via CONVENTIONAL SOLID-STATE TECHNIQUE

I.A. Auwalu^{1*}, H.U. Jamo¹, D.G. Diso¹, A.F. Inuwa¹, M. A. Hotoro¹, A. Aminu² and M. Alhassan³

¹Department of Physics, Faculty of Science, Kano University of Science and Technology, Wudil P.M.B.3244 Kano-Nigeria

²Department of Chemistry, Faculty of Science, Kano University of Science and Technology, Wudil P.M.B.3244 Kano-Nigeria

³Department of Physics, Faculty of Science, Ahmad Bello University, Zaria

ARTICLE INFO

ABSTRACT

Keywords:

Willemite, Optical properties, Samarium Oxide

* Corresponding

Author:

*Corresponding

Author:

futuloli@gmail.com

In this work optical properties of zinc silicate (willemite) glass ceramics doped with samarium oxide at different weight concentrations were determined. The melt quench technique was used to synthesis the samples, with waste rice husks as the silicate source. The energy band gap of samarium doped willemite glass ceramics decreased with increase of samarium dopant concentrations. This indicated the absorption of ultraviolet radiation by the samples. The photoluminescence measurements revealed the red emission which corresponded to the ${}^4G_{5/2} \rightarrow {}^6H_{11/6}$ (646.71 nm) under the blue excitation.

INTRODUCTION

Amidst the frequent host luminescent materials, zinc silicate (Zn_2SiO_4) is known as a suitable host matrix to integrate with rare earth ions and transition metal ions developing in a first luminescence region in blue, green and red spectra (Reddy et al., 2014). In modern technology, rare earth ions are better dopants for light activators in the host matrix materials than transition metals. The outermost orbitals of 5S_2 and 5P_6 completely sheltered the filled 4f shells. The emission changes supply high-pitched lines in the optical spectra accommodating phosphors with excessive luminescence efficiency. Moreover, the rare earth (RE) ions have drawn attention to substituting as an efficient ion in many optical materials due to their large number of absorption and emission bands surfacing from the transitions within the energy levels. Given these factors, many scientists focused their interest on trivalent samarium ions as

luminescence centers in deep red emission arising from conduction band ${}^4G_{5/2} \rightarrow {}^6H_{9/6}$ transition (Sánchez-Royo et al., 2014). Currently, the samarium (Sm^{3+}) ion is one of the most attractive and Valuable rare-earth dopants considering Sm^{3+} -doped phosphors are common to be favorable materials for optical amplifiers, lasers, and electroluminescent devices. Several approaches have been grown to prepare $Zn_2SiO_4: Sm^{3+}$ such as sol-gel synthesis, spray pyrolysis, co-precipitation synthesis, conventional solid-state reaction and hydrothermal method. As a contrast, the stable states technique aims a better clarity in the industrial application than sol-gel method. However, this technique regularly used very cost in SiO_2 source to synthesize the zinc silicate. To overwhelm the disadvantage, it requires changing new silicate sources from waste rice husks silica (WRHS) glasses for expense saving.

The husks silicate glass established to be an appropriate optical material with prominent transparency, excellent rare-earth ion solubility, high thermal stability, and low melting point. Hence, this paper intends to study the synthesis and optical properties of Sm^{3+} doped Zn_2SiO_4 host matrix by adopting an inexpensive solid-state reaction method. Effects of Sm_2O_3 variation concentration in Zn_2SiO_4 (willemite) on the structural and optical properties were investigated.

METHODOLOGY

The conventional solid-state technique was used to produce $(70-X)\text{Zn}_2\text{XSm}_3\text{SiO}_4$ based glass ceramics. The doping proportions were 1, 3 and 5wt% of the samarium oxide REacton 99.9 %. Zinc oxide 20 nm particle size with 99.5% purity was mixed with 63-micron mesh of silica. The silica was acquired from waste rice ash. The mixing procedure was carried out for 24 hours with low energy ball milling. The mixture was heated in a furnace at 1500°C for six hours. The molten mixture was quenched in water and formed a glass fritz at room temperature (Syamimi et al., 2014). Then the glass fritz was crushed and sieved with 63 microns mesh. Polyvinyl alcohol (PVA) acted as a binder to the samples powder. The

sample powder was turned to pellets, with 3.5 tons of pressure for 5 min and sintered at temperatures of 1000°C . At room temperature, Shimadzu UV– visible spectroscopy performed absorption spectra measurements in the range of 217.49–800 nm wavelengths. The optical band gaps of the material was analyzed the sample absorption edges. At room temperature, Perkin Elmer LS 55 Fluorescence spectrometer was used for photoluminescence excitation and emission spectra measurements.

RESULTS AND DISCUSSION

Optical absorption measurements

The optical absorbance of $(70-X)\text{Zn}_2\text{XSm}_3\text{SiO}_4$ was characterized by UV–Vis spectroscopy in Figure 1 revealed the absorption spectra of samarium oxide doped Zn_2SiO_4 in the spectral zone of 220 to 800 nm at room temperature. The shifting of the absorption band to the lower wavelength agreed to the decrease in non-bridging oxygen preparing the structure to be more compact. The absorption spectra of the samples were improved due to dispersing of Zn_2SiO_4 in the crystals lattice (Amjad et al., 2012).

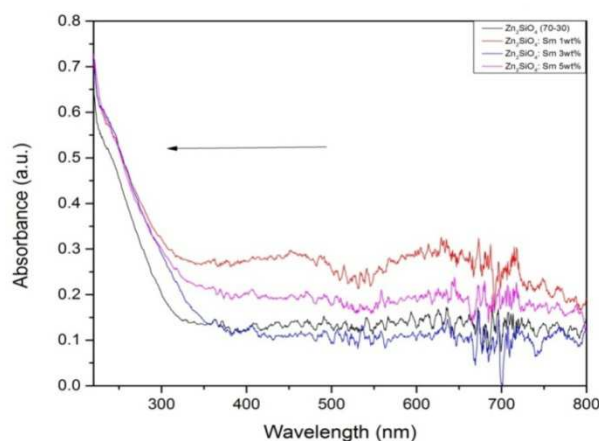


Figure 1. Absorption spectra of $(70-X)\text{Zn}_2\text{XSm}_3\text{SiO}_4$ at $X = 0, 1, 3$ and 5 wt%

Optical band gap

The valence and conduction bands transition of samarium doped Zn_2SiO_4 absorption spectra were accomplished to calculate the band gap (Sahu et al. 2015). The UV–Vis

spectrum of the pure Zn_2SiO_4 crystal was predicted to have a band gap of 5.5 eV. Figure 2 showed that the undoped Zn_2SiO_4 had the band gap energy (E_g) of 3.88 eV before the samarium addition. In the event of Zn_2SiO_4 ,

the indirect transition connection between incident photon energy ($h\nu$) and absorption coefficient (α) had a typical relation²⁵: $(\alpha h\nu)^{1/2} = k [h\nu - E_g]$. Where k is proportionality constant and E_g was the material optical energy band gap. The direct

band gap values were extrapolated from the linear portion of the absorption curves. The variations of dopants concentrations of 1, 3 and 5 wt% yielded the energy band gaps of 3.29, 3.48 and 3.20eV respectively.

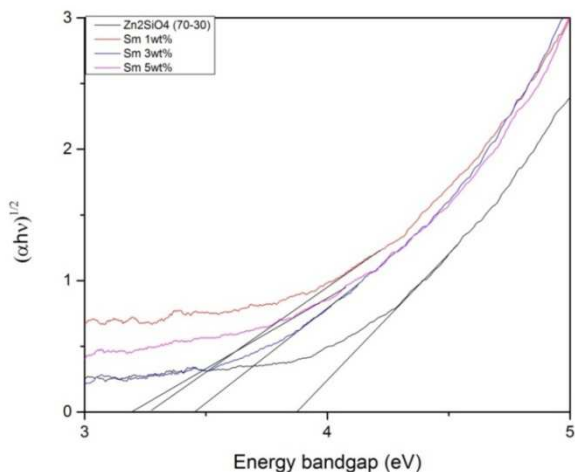


Figure 2. Optical band gap of (70-X) Zn₂XSm₃₀SiO₄ at X =0, 1, 3 and 5 wt%

Figure 3 exhibited the differences of the energy band gap, with different dopant concentrations of (70-X) Zn₂XSm₃₀SiO₄. The energy band gap decreased linearly as the concentration of samarium oxide increased to the pure Zn₂SiO₄. The higher the dopant concentrations led to the increase of non-bridging oxygen and reduced the bridging oxygen. The absorption band tended to move

toward the higher wavelength. In this regard, the sample navigated toward the lower frequency and energy respectively. The increase of the dopant concentrations led to the broadening of impurity band and reduced the energy band gap(Sharma & Bhatti, 2009). The broadening impurity band was simply the band that was located in between valence and conducting band(Erdinc et al., 2010).

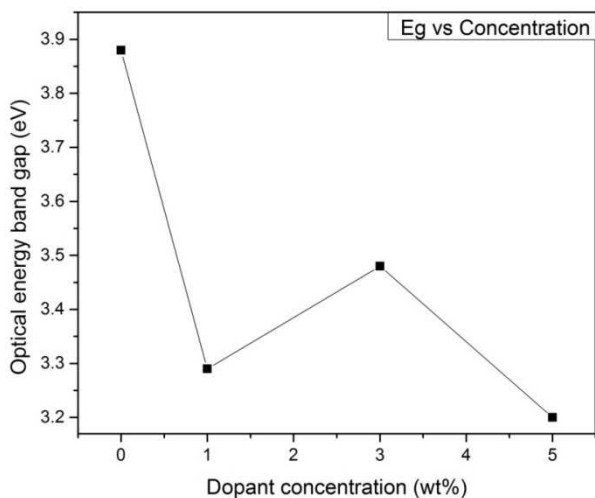


Figure 3. Variations samarium oxides dopant concentrations against optical energy band gap

Photoluminescence

The photoluminescence excitation results for (70-X) Zn₂XSm₃₀SiO₄ were shown in Figure 4. The excitation spectra demonstrated four important peaks at 362.26, 376.80, 389.61 and 406.80 nm with the ground state (⁴G_{5/2}) transitions indicating excited levels. The excitation of 4f-f levels of Sm³⁺ were occupied because of energy transfer from the excited

level to the triplet level, which was employed by rapid intersystem crossing (Bakier 2005). The major peak was positioned at 406.80 nm because of the transitions from ⁶H_{5/6} → ⁴G_{5/2}. The samples experienced high reduction of Luminescence intensity due to quenching effect that occurred in the glass matrix. The addition of Sm³⁺ ions led to the increase of the phonon energy.

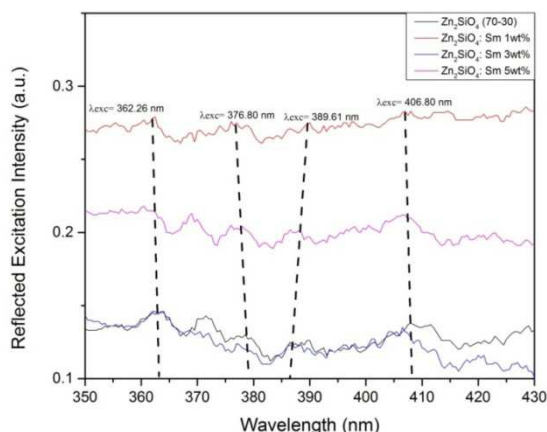


Figure 4. Excitation spectra of (70-X) Zn₂XSm₃₀SiO₄ at X = 0, 1, 3 and 5 wt%

The peak verified Sm³⁺ emission spectra (Fig.5) The blue light (406.80 nm) excitation disclosed four emission spectral bands at 570.50, 595.11, 622.09 and 646.71 nm that were accredited to (⁴G_{5/2} → ⁶H_{5/6}), (⁴G_{5/2} → ⁶H_{7/6}), (⁴G_{5/2} → ⁶H_{9/6}) and (⁴G_{5/2} → ⁶H_{11/6}) respectively. The red shift emission peak originated at 646.71 nm (⁴G_{5/2} → ⁶H_{11/6}) which was ascribed

to the conscious electric dipole transitions of Sm³⁺. Hence, the peak at 570.11 nm (⁴G_{5/2} → ⁶H_{5/6}) was accredited to magnetic dipole transitions (Marzouk et al., 2015). As shown in Figure 5., the emission intensity of (⁴G_{5/2} → ⁶H_{11/6}) transition was decreased due to broken effect of the sample (Brunold, C.T., Gudel, H.U., Cavalli, 1996).

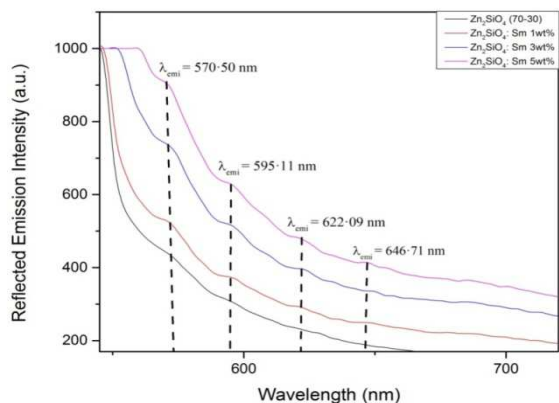


Figure 5. Emission spectra of (70-X) Zn₂XSm₃₀SiO₄ at X = 0, 1, 3 and 5 wt%

CONCLUSION

A melt quench technique was successfully used to synthesize Sm^{3+} doped Zn_2SiO_4 with different weight concentrations. The photoluminescence revealed a red emission at 646.71 nm because of the Sm^{3+} intra ionic transitions at 406.80 nm excitation. The broadening figures of the excitation and

emission spectra were showing the high quenching yield of the sample, which led to the broken effect.

Acknowledgements

The authors greatly acknowledged the financial support from the Tertiary Educational Development fund (TETFund) of Nigeria.

REFERENCES

- Amjad, R.J. et al., (2012). Optical Investigation of Sm^{3+} Doped Zinc-Lead-Phosphate Glass. *Chinese Physics Letters*, 29(8), p.87304. Available at: <http://stacks.iop.org/0256-307X/29/i=8/a=087304?key=crossref.27a11f31c7f9a59f550061c480ecf95d>.
- Ayuni, J.N. et al.,(2011). Optical Properties of Ternary TeO_2 - B_2O_3 - ZnO Glass System. *IOP Conference Series: Materials Science and Engineering*, 17(FEBRUARY), p.12027. Available at: <http://stacks.iop.org/1757-899X/17/i=1/a=012027?key=crossref.2c5543f1d9f886655b515a74d57f4e43>.
- Bakier, E., (2005). Factors affecting light energy transfer in some samarium complexes. *International Journal of Photoenergy*, 7(1), pp.1–8.
- Brunold, C.T., Gudel, H.U., Cavalli, E., (1996). Absorption and luminescence spectroscopy of Zn_2SiO_4 willemitte crystals doped with Co^{2+} . *Chemical Physics Letters*, 252(April), pp.112–120.
- Erdinc, B., Akkus, H. & Goksen, K., (2010). Electronic and optical properties of GaS : A first- principles study. *Optimization*, 23(4), pp.413–422.
- He, H. et al.,(2015). Controllable synthesis of $\text{Zn}_2\text{GeO}_4:\text{Eu}$ nanocrystals with multi-color emission for white light-emitting diodes. *J. Mater. Chem. C*, 3(21), pp.5419–5429. Available at: <http://xlink.rsc.org/?DOI=C5TC00844A>.
- Marzouk, M. a. et al.,(2015). Photoluminescence and spectroscopic dependence of fluorophosphate glasses on samarium ions concentration and the induced defects by gamma irradiation. *Journal of Luminescence*, 166, pp.295–303. Available at: <http://linkinghub.elsevier.com/retrieve/pii/S0022231315003087>.
- Matori, K.A. et al.,(2009). Producing Amorphous White Silica from Rice Husk. *MASJUM Journal of Basic and Applied Sciences*, 1(3), pp.512–515.
- Publishing, I. et al.,(2014). Sensors & Transducers Synthesis and Luminescence Properties of Yellow-emitting. *Sensors & Transducers*, 27(May), pp.295–298.
- Rabiee, S.M. et al.,(2015). Effect of ion substitution on properties of bioactive glasses: A review. *Ceramics International*, 41(6), pp.7241–7251. Available at: <http://www.sciencedirect.com/science/article/pii/S0272884215003818>.
- Reddy, C.P., Naresh, V. & Babu, B.C., (2014). Photoluminescence and Energy Transfer Process in $\text{Bi}^{3+}/\text{Sm}^{3+}$ Co-Doped Phosphate Zinc Lithium Glasses. *Advances in Materials Physics and Chemistry*, 4(September), pp.165–171.
- Sahu, I.P., Bisen, D.P. & Brahme, N., (2015). Structural characterization and optical properties of $\text{Ca}_2\text{MgSi}_2\text{O}_7:\text{Eu}^{2+},\text{Dy}^{3+}$ phosphor by solid-state reaction method. *Luminescence*, 30(5), pp.526–532. Available at: <http://doi.wiley.com/10.1002/bio.2771>.
- Sánchez-Royo, J.F. et al., (2014). Electronic structure, optical properties, and lattice dynamics in atomically thin indium selenide flakes. *Nano Research*, 7(10), pp.1556–1568. Available at: <http://link.springer.com/10.1007/s12274-014-0516-x>.

- Sharma, P. & Bhatti, H.S., (2009). Laser induced down conversion optical characterizations of synthesized $Zn_{2-x}Mn_xSiO_4$ ($0.5 \leq x \leq 5 \text{ mol\%}$) nanophosphors. *Journal of Alloys and Compounds*, 473(1-2), pp.483-489. Available at: <http://linkinghub.elsevier.com/retrieve/pii/S0925838808009444>.
- Sreedhar, V.B., Basavapoornima, C. & Jayasankar, C.K., (2014). Spectroscopic and fluorescence properties of Sm^{3+} -doped zincfluorophosphate glasses. *Journal of Rare Earths*, 32(10), pp.918-926.
- Syamimi, N.F. et al.,(2014). Effect of sintering temperature on structural and morphological properties of europium (III) oxide doped willemite. *Journal of Spectroscopy*, 2014(DECEMBER 2014), pp.1-9.
- Wu, S. et al.,(2015). Effect of TiO_2 Doping on the Structure and Microwave Dielectric Properties of Cordierite Ceramics. *Journal of the American Ceramic Society*, 98(6), pp.1842-1847. Available at: <http://doi.wiley.com/10.1111/jace.13549>.
- Yue, Z. et al.,(2009). Phase Characterization and Dielectric Properties of Zn_2SiO_4 Ceramics Derived from a Sol-Gel Process. *Ferroelectrics*, 387(1), pp.184-188. Available at: <http://www.tandfonline.com/doi/abs/10.1080/00150190902967030>.